Quinoline–dihydropyrimidin-2(1*H*)-one hybrids: Synthesis, biological activity and mechanistic studies

Parth,[a] Hardeep Kaur,[a,b] Leentje Persoons,[c] Graciela Andrei[c] and Kamaljit Singh*[a]

[a] Prof. Dr. Kamaljit Singh, Parth, Dr. Hardeep Kaur
Department of Chemistry, Centre of Advanced Study,
Guru Nanak Dev University,
Amritsar 143 005, India
E-mail: kamaljit.chem@gndu.ac.in
[b] Dr. Hardeep Kaur
PG Department of Chemistry,
Khalsa College,
Amritsar 143 005, India
[c] Dr. Leentje Persoons, Dr. Graciela Andrei
KU Leuven Department of Microbiology, Immunology and Transplantation,
Laboratory of Virology and Chemotherapy,
Rega Institute, Leuven, Belgium

Supporting information for this article is given via a link at the end of the document.

Abstract A novel class of quinoline–dihydropyrimidin-2(1*H*)-one (DHPM) hybrids was synthesized and *in vitro* antiplasmodial activity was evaluated against chloroquine sensitive (D10) and chloroquine resistant (Dd2) strains of *Plasmodium falciparum*, the human malaria parasite. The antiplasmodial activity was compared to previously reported DHPM based molecular hybrids. Dual mode of antiplasmodial action of the most active member has been evaluated through heme binding study and *in silico* docking in the active site of dihydrofolate enzymes (wild-type as well as mutant). Favourable pharmacokinetic parameters were predicted in the ADMET evaluation. The new hybrids were also tested against a number of DNA and RNA viruses. No antiviral activity was found, except for one hybrid that showed mild inhibitory activity against two strains of cytomegalovirus (AD-169 and Davis), The most active hybrid was found to be a selective inhibitor of the growth of *P. falciparum* as well as a modest inhibitor of varicella zoster virus in HEL cells. Cytotoxicity of all hybrids was assessed in HEL, HeLa, Vero, MDCK, and CRFK cell cultures.

Introduction

Malaria remains as a major public health threat as it is responsible for about half a million deaths annually throughout tropical endemic regions.[1] Over 241 million cases of malaria were reported in 2020 alone and the incidence of malaria has not seen a significant decrease over the years.[2] In the year 2020, more than 90% of all malaria cases and 96% of all malaria related deaths were reported in the sub-Saharan African region. Children under the age of 5 years were the most affected as they accounted for more than 80% of all reported deaths.[2] Human malaria is caused by five species (*P. falciparum, P. vivax, P. ovale, P. malariae and P. knowlesi*) of the genus *Plasmodium*.[1,3] However, the first two account for, respectively 90% and 10% of all malaria cases including complicated malaria.[4] The clinical symptoms of malaria appear during the asexual stages of *Plasmodium*. Transmission of parasites from humans to mosquitoes relies on gametocytes, a specialized class of sexual cells, which mature through five morphologically different developmental stages in about ten days.[5] An effective strategy for eradication of malaria should thus target not only the asexual stages, but also the transmission stage.[6]

The key approaches that are implemented to manage malaria include (i) preventive measures, e.g. through the use of insecticidal treated bed nets and mosquito repellent indoor sprays,[7] (ii) provision of seasonal malaria chemoprevention, through monthly administration of antimalarial drugs[8] and (iii) treatment of malaria infection by antimalarial drugs.[9] Very recently in October 2021, the World Health Organization (WHO) has recommended the use of malaria vaccine, RTS,S/AS01 (RTS,S) among children in sub-Saharan Africa and in regions with moderate to high *P. falciparum* malaria transmission.[10] However, efforts to develop vaccines against *P. vivax* are only limited,[11] despite the enormous burden caused by this parasite species.

The development of resistance in *P. falciparum* and *P. vivax* to almost all front-line antimalarial drugs such as sulfadoxine/pyrimethamine (Pyr), mefloquine, halofantrine, and quinine has posed one of the biggest threats to malaria control and has led to increased malaria morbidity and mortality.[12] Gene mutations often associated with the development of resistance in malaria parasites, are accountable for a significant drop in the ability of antimalarial drugs to cure malaria.[12] The emergence and spread of *P. falciparum* parasites with

diminished susceptibility to artemisinin derivatives has raised concerns regarding the efficacy of currently available antimalarial drugs. Consequently, artemisinin combination therapies (ACTs),[13,14] which comprise artemisinin and a partner drug have also shown signs of resistance as indicated by the treatment failures with ACTs. This is a major wake-up call to find alternative drugs or treatment strategies to avoid mushrooming of the "super resistant" parasites.[15] Since development of resistance to antimalarial drugs is obvious and cannot be completely eliminated, there is a dire need to identify new antimalarial pharmacophores, without going into extensive structure-activity relationships (SARs), which can be done at the later development stage. At the same time, there is a need to design drugs, which can target more than one stage of the complex life cycle of malaria parasite, as evidenced by the "hybrid drugs", a strategy that not only provides new drugs but may also potentially delay the development of resistance.[16] In this direction, we[17-20] and others,[21-23] in the past have reported efficacy of several types of rational designs of hybrid drugs and their antimalarial activity.

Substituted 3,4-dihydropyrimidin-2(1*H*)-ones (DHPMs)[24] bearing variable substitution patterns exhibit interesting multifaceted (calcium channel modulators,[25] antihypertensive agents,[26] adrenergic receptor antagonists,[27] mitotic kinesin Eg5 inhibitors,[28] and hepatitis B replication inhibitors[29]) pharmacological profiles. Furthermore, the batzelladine alkaloids A isolated from marine sources containing a DHPM core inhibit the binding of HIV[30] envelop protein gp-120 to human CD4 cells, making them potential new leads for AIDS therapy. Thus, DHPM is a potentially useful pharmacophore for the search of new drugs. Structure diversification of DHPMs has led to the identification of a number of differently substituted DHPMs out of which DHPM derivatives appended with a chloroquine (CQ) based fragment at the N-3 position (**1**, Figure 1) were identified[31] as potent antimalarials with antiplasmodial activity in nanomolar (nm) range against CQ sensitive (CQ^S) 3D7 as well as CQ resistant (CQ^R) K1 strains of *P. falciparum*.

Phosphorodiamidates have come up as a promising new phosphate prodrug motif for antiviral drug discovery.[32] Phosphoramides are isosteres of phosphorodiamidates, a link also used in potent antiviral agents active against chikungunya.[33] During our ongoing research on the synthesis of hybrid antimalarials,[17-20] we realized that incorporation of a phosphoramide link to connect DHPMs and a CQ based fragment may be a good strategy to design new antimalarials, which at the same time could show antiviral activity.

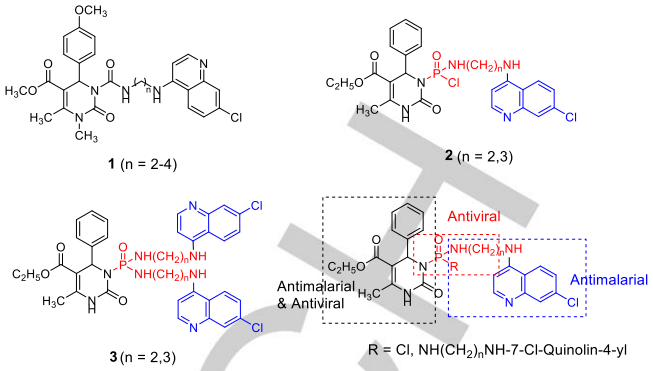

Figure 1. Quinoline -DHPM hybrids **1** and design strategy for phosphoramide hybrids **2** and **3**.

Herein we report the synthesis and characterization of novel quinoline-DHPM hybrids **2-3** (Figure 1) linked through a phosphoramide link. We also report *in vitro* antiplasmodial activity of these hybrids against D10 (CQ^S) and Dd2 (CQ^R) strains of *P. falciparum* and draw comparison with quinoline-DHPM hybrids **1** reported in literature.[31] Since these types of drugs exert antimalarial activity by binding to β-haematin, preventing haemazoin[34] formation in the digestive vacuole (DV) of the parasite and by inhibition of dihydrofolate reductase (DHFR),[20] we have studied binding of the most active compound with heme using UV-visible spectroscopy and mass spectrometry as well as performed docking studies of the most active hybrid in the active site of the wild type *Pf*-DHFR-TS and mutant *Pf*-DHFR-TS.[35] We have also analyzed the pharmacokinetic properties of the compounds using ADMET predictions.[36] Additionally, these hybrids were also evaluated for their antiviral activity.

Results and Discussion

Chemistry

The synthesis of the target quinoline-DHPM hybrids was carried out as shown in Scheme 1. The first step of the synthesis involved standard HCl-catalyzed Biginelli condensation of benzaldehyde, ethyl acetoacetate and urea leading to DHPM **4**. Subsequently, **4** was treated with phosphorous oxychloride ($POCl_3$) to obtain the corresponding dichlorophosphoramide derivative **5**. Nucleophilic substitution reaction of **5** with appropriate 4-amino-7-chloroquinoline **6** in dioxane at 0 °C yielded quinoline-DHPM hybrids **2a**-**b** and **3a**-**b**. Structures of **2**-**5** were established on the basis of spectral (^{1}H NMR, ^{13}C NMR, ^{31}P NMR, HRMS, FTIR) (See Supporting information, Figs S1-S12) as well as microanalytical analysis.

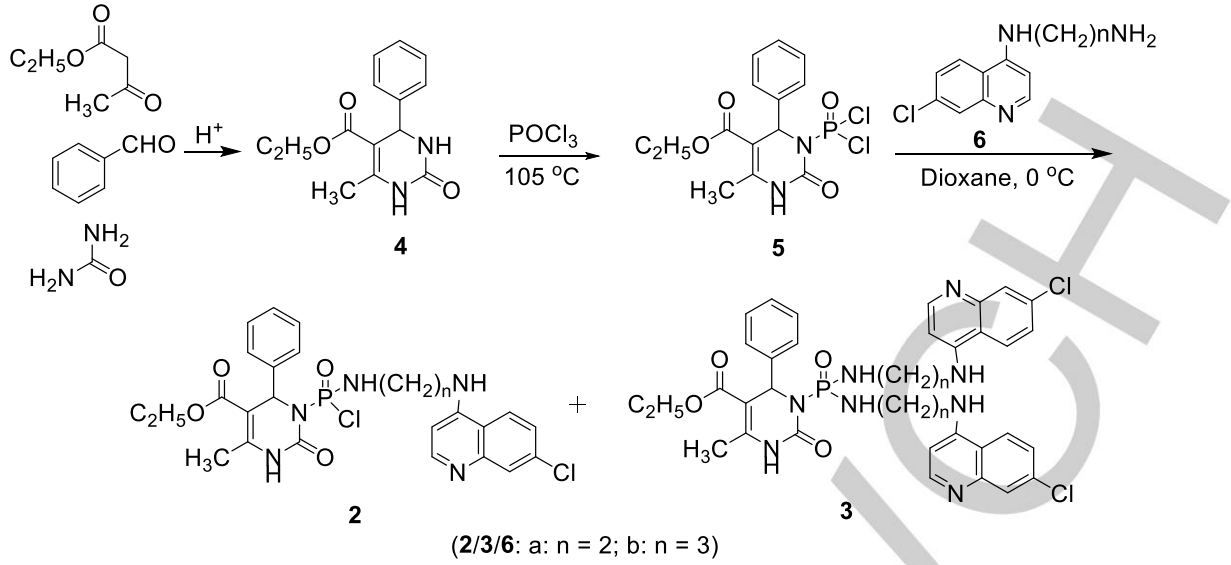

Scheme 1. Synthesis of quinolone-DHPM phosphoramide hybrids **2**/**3**.

***In vitro* antiplasmodial activity**

The in vitro antiplasmodial activity of **2**-**3** (Table 1) was determined against D10 (CQ^S) and Dd2 (CQ^R) strains of *P. falciparum*. Initially, parasite survival (Table 2) for the synthesized hybrids **2**-**3** was determined at different concentrations: 10 µg/ml, 5 µg/ml and 2.5 µg/ml. The hybrids inhibited the parasite survival to a different extent at all the three tested concentrations. Except for **2a**, the percent survival of the parasite at the lowest of the three concentrations used was less compared to the parasite survival at the highest (30 ng/mL) concentration of the reference drug CQ. Furthermore, the half maximal inhibitory concentration (IC_{50}) of hybrids **2**-**3** were calculated against CQ^S (D10) and CQ^R (Dd2) strains and are summarized in Table 1. Evidently, the diaminoquinoline hybrids (**3a**-**b**) have antiplasmodial activity in the lower µM range against both CQ^S and CQ^R strains of *P. falciparum*. The antiplasmodial activity data showed that diamino substituted hybrids **3a** and **3b** are more active in comparison to hybrids **2a** and **2b** having one aminoquinoline group. Furthermore, increasing the number of methylene groups from two (**2a**, **3a**) to three (**2b**, **3b**) resulted in an increase in the antiplasmodial activity against both CQ^S and CQ^R strains. Thus, the hybrids bearing three methylene spacers were more effective. The hybrid **3b** (IC_{50} = 0.285 µM) was identified as the most potent hybrid, having an antiplasmodial activity comparable to CQ (IC_{50} = 0.138 µM) against the Dd2 CQ^R strain.

We also took the opportunity to compare the activity of this set of hybrids with the DHPM-quinoline hybrids **1a-c**, reported earlier[33] against CQ^S (3D7) and CQ^R (K1) strains of *P. falciparum*. These hybrids are also based on a DHPM core, yet the substitution pattern is different. When evaluating against different *Plasmodium* strains, the antiplasmodial activity of **1a-c** was marginally superior to the **2-3** hybrids.

The cytotoxicity of these hybrids was assessed in CRFK (Table 1), HeLa, Vero, and HEL cell cultures (See Supporting information, Tables S1-S6). Except for **3b**, all CC_{50} values were greater than the highest concentration tested (100 µM), providing a promising selectivity window. The therapeutic index (TI, Table 1) was determined from the ratio of CC_{50} (µM) and *in vitro* antimalarial activity (IC_{50} in µM for Dd2 strain). Hybrid **3b**, the most active member of the current series exhibited a high TI and can be seen as good lead for further structure modification.

Mode of action studies

Heme binding studies

The principal mode of action of the quinoline antimalarials (e.g. CQ, amodiaquine and quinine etc.) is through blocking of the hemazoin formation. This is achieved by forming adducts with ferriprotoporphyrin IX. We have evaluated the heme [Fe(III)PPIX] binding proficiency and the consequent inhibition of β-haematin formation of **3b**, the most potent member of the current set in solution using UV-visible spectrophotometer.[17,37] Incremental addition of a solution of **3b** (0.05−28 µM, DMSO) into a constant concentration of monomeric heme (2.4 µM, DMSO:H_2O/4:6, *v/v*) in 0.02 M HEPES buffer (pH 7.4), resulted in a substantial decrease in intensity of the Fe(III) PPIX Soret band at 402 nm without a shift in the absorption maximum (Figure 2). The titration was also performed at the acidic pH 5.6 (0.02 M MES buffer in aqueous DMSO), corresponding to the digestive vacuole (DV) of the parasite.

Table 1. *In vitro* antiplasmodial activity of **2**-**3** against *P. falciparum* strains (CQ^S) D10 strain and (CQ^R) Dd2 (**2**,**3**) (n = 3) and (CQ^S) 3D7 strain and (CQ^R) K1 (**1a**-**c**, n = 2,3,4 respectively) (n = number of replicates).

Code	Compound[a]	D10/3D7 IC_{50} (μM)	Dd2/K1 IC_{50} (μM)	CC_{50} (μM)[b]	TI[c]
2a	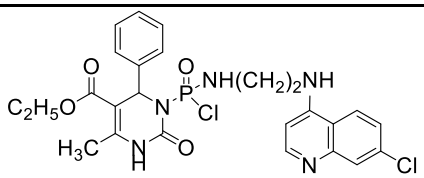	5.008	ND	>100	-
3a	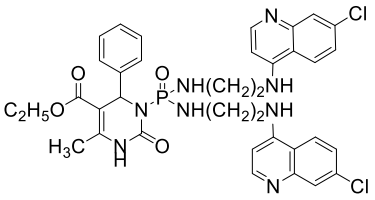	0.571	0.527	>100	-
2b	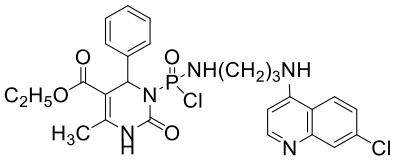	1.856	ND	>100	-
3b	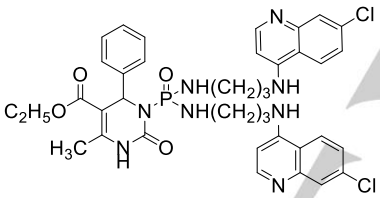	0.514	0.285	49.1	172.3
1a	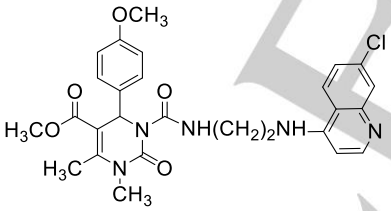	0.032	0.131	31.40	240
1b	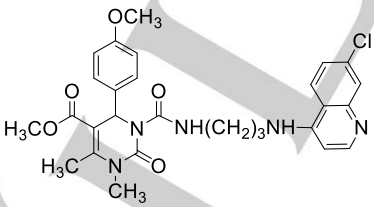	0.062	0.144	26.97	187
1c	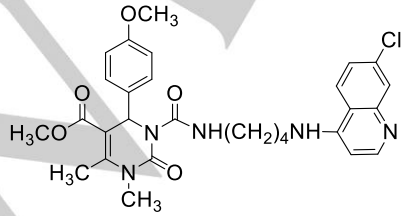	0.007	0.008	4.97	621
CQ		0.021[d]	0.138[e]	-	-

[a] Taken from ref. 31. [b] 50% Cytotoxic concentration determined on Crandell-Rees Feline Kidney cells (CRFK) cells by measuring the cell viability with the colorimetric formazan- based MTS assay. [c] Therapeutic index is calculated as CC_{50}/ IC_{50} (Dd2/K1 Strain) ratio. [d] n = 40. [e] n = 6. ND = not determined.

Table 2. Parasite survival (%) of hybrids **2-3** against D10 strain.

Compound	% Parasite survival[a] 10 µg/mL	5 µg/mL	2.5 µg/mL
2a	16.8	28.2	50.1
3a	5.4	9.3	10.5
2b	14.1	14.5	27.4
3b	3.6	5.9	10.8
CQ[b]	30.1[c]	46.9[d]	88.8[e]

[a] Mean of three determinations. [b] n = 12 (concentrations used: [c] 30 ng/mL [d] 15 ng/mL [e] 7.5 ng/mL).

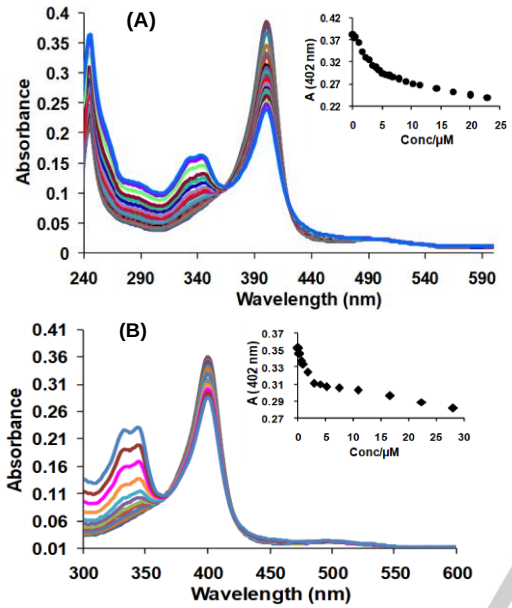

Figure 2. (A) Titration of **3b** with monomeric heme at pH 7.4; (B) Titration of **3b** with monomeric heme at pH 5.6.

The binding of **3b** with heme at the experimental pH was not affected by DMSO used as solvent. The Job's plot (Supporting Information, Figure S13) revealed a 1:1 stoichiometry of the most stable complex of **3b** with monomeric heme at both, pH 7.4 and 5.6. Further, analyzing the titration curves obtained at pH 7.4 using HypSpec, a nonlinear least-squares fitting program,[38] furnished association constants reported in Table 3.

A similar titration of CQ with heme was also performed at the pH values used for **3b** and the binding constants were calculated to draw comparisons. The data provided in Table 3 shows that the association constant (log K 5.55) calculated for the complexes of monomeric heme and **3b** is greater than that of CQ and heme (log K 4.65). Furthermore, the binding constant data (Table 3) show that the binding is stronger even at acidic pH as upon decreasing the pH from 7.4 to 5.6, insignificant effect on the binding constants was seen.

Using a standard procedure,[39] the binding of **3b** with µ-oxo dimer of heme was also studied at pH 5.8. Thus, stepwise addition of **3b** (0.2−30 µM) was made to a solution of µ-oxo

Table 3. Binding constant (log *K*) of **3b** and CQ with heme and µ-oxo heme.

Compound	Monomeric heme Log *K* ±σ		µ-Oxo heme Log *K* ±σ
	pH 5.6	**pH 7.4**	**pH 5.8**
3b	5.55 ± 0.04	5.36 ± 0.02	5.17 ± 0.05
CQ	4.650 ± 0.02	5.15± 0.10	5.58± 0.08
Stoichiometry	1:1	1:1	1:1

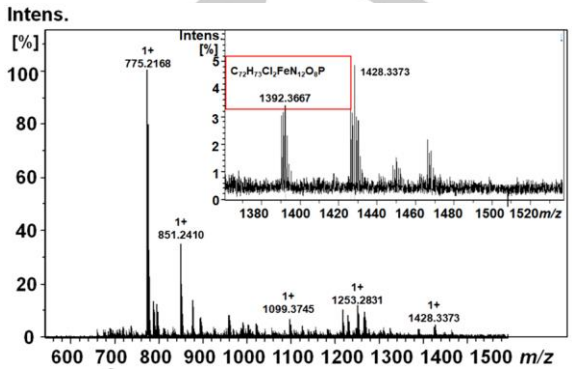

Figure 3. The solution phase mass spectra of **3b** (20 µM) upon addition of monomeric heme (20 µM) in 40% aqueous DMSO solution.

heme (10 µM) in phosphate buffer (20 mM) at pH 5.8 and the attendant change (decrease) in the absorbance at 364 nm (Supporting Information, Figure S14A) was noticed. A 1:1 stoichiometry was reflected by the Job's plot for the most stable µ-oxo: **3b** complex (Supporting Information, Figure S14B). The association constants (calculated using HypSpec) suggested that the binding of **3b** with monomeric heme (log K 5.55) is stronger than both, the µ-oxo heme (log K 5.17) as well as the reference drug CQ (log K 4.65). Thus, **3b** is proposed to inhibit hemozoin formation by blocking the growing face of heme, which is also correlated with the antiplasmodial activity. Furthermore, the mass spectra of an equimolar (20 µM) solution of **3b** and hemin chloride showed a peak at 1392.42 Da (Figure 3), corresponding to the molecular formula $C_{72}H_{73}Cl_2FeN_{12}O_8P$. This further indicates the binding of heme with **3b** and formation of a 1:1 complex.

Docking analysis

Pyrimidine based antimalarials such as Pyr are inhibitors of malarial dihydrofolate reductase (DHFR). The modes of binding of Pyr to wild type and mutant DHFRs have led to the identification of the molecular basis for resistance against Pyr and to the rational design of new effective inhibitors. Thus, *in silico* docking studies of the most active member **3b** were performed in the binding pocket of both the wild type *Pf*-DHFR-TS (PDB ID: 3QGT) and quadruple mutant of *Pf*-DHFR-TS (N511, C59R, S108N, I164 L; PDB ID: 3QG2)[35]

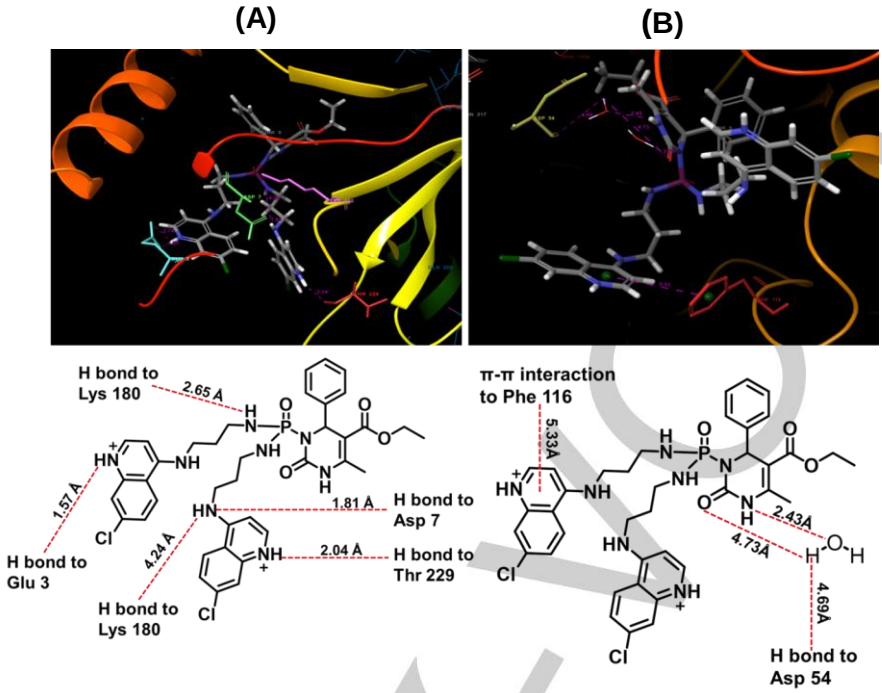

Figure 4: 2D and 3D docking poses of compound **3b** showing interaction in the binding sites of (A) wild type *Pf*-DHFR-TS (PDB ID: 3QGT) and (B) quadruple mutant (N511+C59R+S108N+I164L) *Pf*-DHFR-TS (PDB ID: 3QG2).

Table 4. Glide docking score and docking energies (Kcal/mol) of **3a** and the reference DHFR-inhibitors bound to wild type and mutant *Pf*-DHFR-TS binding site.

	Wild type *Pf*-DHFR-TS[a]		Mutant *Pf*-DHFR-TS[b]	
	SP GScore	**Glide Energy**	**SP GScore**	**Glide Energy**
3b	-4.77	-47.99	-9.13	-72.90
Dihydrofolate[c]	-7.28	-49.39	-9.66	-63.39
Pyrimethamine[c]	-3.28	-21.89	-7.68	-38.55
Cycloguanil[c]	-3.76	-24.41	-6.25	-34.76
WR99210[c]	-4.02	-26.33	-7.63	-40.82

a] PDB ID: 3QGT. [b] PDB ID: 3QG2. [c] Data for SP level calculations.

structures using Schrödinger_Suites_2021-3, LLC, NY, 2021.

The binding energy of **3b** (47.99 Kcal/mol and 72.90 Kcal/mol respectively) towards wild-type and quadruple mutant *Pf*-DHFR-TS structures was greater than the binding energy of Pyr as well as the standard *Pf*-DHFR inhibitors (cycloguanil and WR99210) and comparable to the native substrate, dihydrofolate (Table 4). Compound **3b** shows different poses in both the wild type and quadruple mutant and shows different interactions as it binds (Figure 4) deep in the binding pocket of the mutant Pf-DHFR forming a major π-π interaction (5.33 Å) between the aromatic ring of Phe116 with the aromatic ring of the chloroquinoline unit of **3b**. The carbonyl group of the pyrimidine ring forms a hydrogen bonding interaction (4.73 Å) with water, which is also linked through a hydrogen bond (4.69 Å) with the carbonyl group of Asp54. Similarly, NH of the pyrimidine ring shows hydrogen bonding (2.43 Å) with water. While in wild type *Pf*-DHFR, Glu3 residue formed a hydrogen bond with protonated (pH 5 – 7) nitrogen atom of aminoquinoline moiety (Glu3 CO···HN: 1.57 Å). Similarly, Asp7 formed a hydrogen bond with amine NH of aminoquinolines moiety (Asp7 CO···HN: 1.81 Å), additionally, a hydrogen bond is also formed with the Lys180 (NH···N: 4.24 Å). Interestingly, the P atom of the phosphoramide link attached to the pyrimidine ring formed a hydrogen bond with Lys180 (NH···O=P: 2.65 Å). Likewise, Thr229 formed a hydrogen bond with the protonated quinoline ring nitrogen atom of aminoquinolines moiety as previously

Table 5. Predicted ADMET properties of compounds.

Compound	% HIA[a]	Caco-2 Per[b]	FU[c]	BBB Per[d]	CNS Per[e]	CYP3A4[f]	CL tot[g]	AMES toxicity	LD_{50} (mol/kg)[h]
2a	91.326	0.677	0	-1.577	2.403	Yes	-0.054	No	3.167
3a	87.384	0.748	0.032	-1.825	-3.394	Yes	-0.028	No	3.042
2b	92.207	0.692	0	-1.63	-2.332	Yes	-0.086	No	3.172
3b	89.158	0.692	0.07	-2.014	-3.104	Yes	-0.087	No	2.932
WR99210	80.25	0.666	0.607	-1.694	-3.443	Yes	0.313	No	2.447
Pyr	92.345	1.157	0.278	0.188	-2.231	No	-0.031	No	2.865
Cycloguanil	92.262	0.642	0.307	-0.618	-3.219	No	0.251	No	2.52

[a] % HIA, human intestinal absorption (>30% readily absorbed). [b] Caco-2 Per (log Papp in 10^{-6}cm/s), Caco-2 permeability (>0.90 readily permeable). [c] FU, Fraction unbound (human). [d] BBB Per, Blood brain barrier permeability (log BB). [e] CNS Per (log PS), Center nervous system permeability (log PS> - 2 penetrate the CNS, log PS < -3 unable to Penetrate CNS). [f] Substrate & inhibitor. [g] CLtot (log mL/min/kg), total clearance. [h] LD_{50}, Oral rat acute toxicity.

Table 6. Prediction of Lipenski's rule of 5 and drug-likeness score.

Compound	Mass (<500)	H-bond acceptor (<10)	H-bond donor (<5)	Log P (<5)	Drug likeness (>0)	Violation
2a	562.38	6	3	3.78	1.19	1
3a	747.61	8	5	4.76	1.19	2
2b	576.41	6	3	3.98	1.13	1
3b	775.66	8	5	5.43	1.13	2

mentioned (Thr229 CO$\cdots$HN: 2.04 Å). Understanding of the interactions of **3b** with the enzyme should aid in the design of more potent inhibitors that bind more tightly and effectively to the mutant enzymes.

ADMET predictions

The pharmacokinetic properties such as absorption, distribution, metabolism, excretion and toxicity (ADMET) including Lipinski's rule of five,[40] drug-likeness of the compounds were predicted using online tools.[36] Lipinski's rule of five, which includes hydrogen bond donor, hydrogen bond acceptor, molecular weight, and solubility parameters were predicted using SWISS ADME. Drug likeness of the compounds was predicted using Molsoft LLC online web server and pharmacokinetics parameters by using *in silico* methods pkCSM (http://biosig.unimelb.edu.au/pkcsm/prediction) web tools.

The absorption of drugs is deduced from the membrane permeability (indicated by colon cancer cell line, Caco-2), and intestinal absorption (% HIA) (Table 5 and supporting information See Tables S7-S9, and Figure S15). The distribution of drugs is based on the blood–brain barrier (BBB) permeability, fraction unbound and CNS permeability (Table 5). Metabolism is based on the ability of the compounds to be a substrate of CYP3A4 as cytochromes P450 are responsible for metabolism of many drugs, whereas excretion is indicated by the drug clearance measured as CLtot. Finally, toxicity is indicated by AMES toxicity and rat LD_{50} values (Table 5). Thus, while the compounds showed effective human intestinal absorption, the Caco-2 permeability is in the range 0.666-0.748 against >0.9 for the readily permeable drugs. While the distribution parameters of the set of **2/3** are not very favorable, except **2a**, the compounds seem to be good substrates of CYP3A4, indicating their likelihood to metabolism. AMES toxicity and LD_{50} values (Table 5) indicated the compounds to be non-toxic. The predictions of the Lipinski's rule of 5 (Table 6) revealed that **2a** and **2b** violated only one rule, whereas both for **3a** and **3b** two violations were counted. The rule of 5 states that an orally active compound should have no more than one violation from these criteria. However, in medicinal chemistry, an attempt to increase the selectivity and potency of hit compounds often results in an increase in molecular weight, and several orally bio available drugs do not strictly meet the criteria of Lipinski's rule of 5.

Antiviral activity

CQ and DHPMs have antiviral effects against several viruses, including human immunodeficiency virus type 1, HCoV-229E, hepatitis B virus, and herpes simplex virus type 1.[41] Thus, we determined the antiviral activity of the current set of quinolone-DHPM hybrids against a broad panel of viruses, including

Table 7. Antiviral activity of phosphoramide derivatives **2-3** against cytomegalovirus (CMV) and varicella-zoster virus (VZV) in human embryonic lung (HEL) cells.

	Cytomegalovirus (CMV) in human embryonic lung (HEL) cells			varicella-zoster virus (VZV) in human embryonic lung (HEL) cells		
Compound	**EC_{50}[a] (μM)**		**Cytotoxicity (μM)**	**EC_{50}[a] (μM)**		**Cytotoxicity (μM)**
	AD-169 strain	**Davis strain**	**Cell morphology (MCC)[b]**	**TK^+ VZV OKA strain**	**TK^- VZV 07-1 strain**	**Cell morphology (MCC)[b]**
2a	>100	>100	>100	>20	>20	100
3a	>100	>20	>100	>20	>20	100
2b	48.9	54.7	>100	>100	>100	>100
3b	>20	>20	100	10.4	20	100
CQ	>20	>4	>20	>4	>4	>20
Ganciclovir	7.87	5.98	>350	-	-	-
Cidofovir	0.86	1.84	317	-	-	-
Brivudin	-	-	-	3.82	144.9	>440
Acyclovir	-	-	-	0.026	143.6	300

[a] Effective Compound concentration required to reduce virus plaque formation by 50%. Virus input was 100 (HCMV) or 20 (VZV) plaque forming units (PFU). [b] Minimum cytotoxic concentration that causes a microscopically detectable alteration of cell morphology. TK: thymidine kinase.

(i) cytomegalovirus, varicella zoster virus (vzv) in human embryonic lung (HEL) cells (Table 7), (ii) herpes simplex virus-1 (HSV-1; KOS), herpes simplex virus-2 (HSV-2; G), vaccinia virus, vesicular stomatitis virus, herpes simplex virus-1 (TK–KOS ACV^R) in HEL cell cultures, (iii) parainfluenza-3 virus, reovirus-1, Sindbis virus, Coxsackie virus B4, Punta Toro virus in Vero cell cultures, (iv) feline corona virus (FIPV) and feline herpes virus activity in CRFK cell cultures (v) influenza A virus (H1N1 and H3N2) and influenza B virus in MDCK cell cultures, (vi) vesicular stomatitis virus, coxsackie virus B4 and Respiratory syncytial virus infecting HeLa cell cultures. (See supporting information Tables S1-S5).

Among the screened hybrids (as well as CQ), none depicted any significant antiviral activity except for hybrid **2b** and **3b** against CMV and VZV, respectively (Table 7). It should be noted that the anti-CMV activity of the hybrid **2b** was minimal and the hybrid **3b** showed modest activity against both thymidine kinase (TK) wild-type (TK^+) and thymidine kinase deficient (TK^-) VZV strains. Further structure modification is needed to produce compounds with more pronounced antiviral activity.

Conclusion

In this investigation, quinoline–DHPM phosphoramide hybrids with good antimalarial activity were reported. The hybrids **3a**-**b** were found to be more active in comparison to hybrids **2a**-**b**. Among the synthesized hybrids, **3b** exhibited the lowest IC_{50} value against both CQ^S and CQ^R strains of *P. falciparum*. These hybrids were found to be non-toxic in HEL, HeLa, Vero and CRFK cell cultures. Additionally, hybrids **2b** and **3b** showed inhibitory activity against cytomegalovirus and varicella-zoster virus, respectively. The mechanism of the observed antimalarial activity was established in terms of binding with heme. These hybrids can serve as good lead for the synthesis of novel quinoline–DHPM phosphoramide hybrids.

Experimental Section

General

All liquid reagents were dried/purified following recommended drying agents and/or distilled over 4 Å molecular sieves. Dioxane was dried over 4 Å molecular sieves. ^{1}H NMR (400 MHz) and ^{13}C (100 MHz) NMR spectra were recorded in $CDCl_3$ on a multinuclear Jeol FT-AL-400 spectrometer with chemical shifts being reported in parts per million (δ) relative to Internal tetramethylsilane (TMS, δ 0.0, ^{1}H NMR) or chloroform ($CDCl_3$, δ 77.0, ^{13}C NMR). Mass spectra were recorded at Department of Chemistry, Guru Nanak Dev University, Amritsar on a Bruker LC-MS MICROTOF II spectrometer. Elemental analysis was performed on FLASH EA 112 (Thermo electron Corporation) analyzer and the results are quoted in %. IR recorded on Perkin Elmer FTIR-C92035 Fourier transform spectrometer in the range 400-4000 cm^{-1} using KBr pellets. Melting points were determined in open capillaries and are uncorrected. For monitoring the progress of a reaction and for comparison purpose, thin layer chromatography (TLC) was performed on pre-coated aluminum sheets Merck ($60F_{254}$, 0.2 mm) using an appropriate solvent system. The chromatograms were visualized under UV light. For column chromatography silica gel (60-120 mesh) was employed and eluents were ethyl acetate/hexane or ethyl acetate/methanol mixtures. UV-visible spectral studies were conducted on Shimadzu 1601 PC spectrophotometer with a quartz cuvette (path length, 1 cm). The absorption spectra have been recorded between 1100 and 200 nm. The cell holder of the spectrophotometer was thermostatted at 25 °C for consistency in the recordings.

General procedure for the synthesis of ethyl 3-(dichlorophophoryl)-6-methyl-2-oxo-4-phenyl-1,2,3,4-tetrahydropyrimidine-5-carboxylate (5)

Ethyl 6-methyl-2-oxo-4-phenyl-1,2,3,4-tetrahydropyrimidine-5-carboxylate (**4**, DHPM) (0.01 moles) was suspended in phosphorous oxychloride (10 ml) and heated at 105 °C for 45 min. Excess phosphorous oxychloride ($POCl_3$) was removed under reduced pressure and last traces of $POCl_3$ were removed through azeotropic distillation with dry benzene to furnish the 3-dichlorophosphinyl DHPM derivative **5** in 90-95% yield and were used for subsequent reactions without further purification.

General procedure for the reaction of 5 with N^1-(7-chloroquinolin-4-yl)ethane-1,2-diamine 6a and N^1-(7-chloroquinolin-4-yl)propane-1,3-diamine 6b

To the stirred solution of compound **5** (1.0 equiv.) in dry dioxane (10 ml) appropriate amine **6** (2 equiv.) was added and resulting solution was stirred at 0 ºC for 2 h. After completion of reaction (TLC), dioxane was removed under reduced pressure and the residue was purified by column chromatography using ethyl acetate and methanol as eluents. The isolated compounds were recrystallized from chloroform/ hexane.

Ethyl 3-(chloro((2-((7-chloroquinolin-4-yl)amino)ethyl)amino)phosphoryl)-6-methyl-2-oxo-4-phenyl-1,2,3,4-tetrahydropyrimidine-5-carboxylate (2a)

Yellow solid. Rf: 0.86 (60% methanol: ethyl acetate). Yield: 26%. M.p. 180 °C. FTIR (KBr): ν_{max} 1025, 1095, 1238, 1453, 1635, 1704, 2927, 3119, 3306 cm^{-1}. ^{1}H NMR (400 MHz, DMSO, 25 °C): δ 1.25 (t, 3H, *J* 7.3 Hz, CH_3), 2.31 (s, 3H, C6-CH_3), 3.27 (m, 4H, CH_2), 4.17 (m, 2H, ester-CH_2), 6.04 (d, 1H, *J* 5.84 Hz, C4-H), 6.23 (s, 1H, ArH), 6.43 (br, 1H, D_2O exchangeable, NH), 7.23- 7.84 (m, 7H, ArH), 8.44 (m, 2H, ArH), 9.27 (br, 1H, D_2O exchangeable, NH). ^{13}C NMR (100 MHz, DMSO, 25 °C): δ 14.1, 17.2, 40.9, 44.8, 53.6, 58.3, 98.2, 116.6, 122.1, 123.3, 125.4, 126.8, 127.1, 133.1, 143.4, 146.9, 148.1, 149.5, 150.8, 151.9 and 164.4. ^{31}P NMR (162 MHz, DMSO, 25 °C): δ 12.53. Anal. Calcd. for $C_{25}H_{26}Cl_2N_5O_4P$: C, 53.39; H, 4.66; N, 12.44; Found: C, 53.20; H, 4.20; N, 12.12. MS: *m/z* 562 (M^+).

Ethyl 3-(chloro((3-((7-chloroquinolin-4-yl)amino)propyl)amino)phosphoryl)-6-methyl-2-oxo-4-phenyl-1,2,3,4-tetrahydropyrimidine-5-carboxylate (2b)

Yellow solid. Rf: 0.41 (60% methanol: ethyl acetate). Yield: 60%. M.p. 110 °C. FTIR (KBr): ν_{max} 1028, 1097, 1237, 1452, 1633, 1703, 2930, 3119, 3401 cm^{-1}. ^{1}H NMR (400 MHz, DMSO, 25 °C): δ 1.15 (t, 3H, *J* 7.1 Hz, CH_3), 2.28 (s, 3H, C6-CH_3), 2.94 (m, 2H, CH_2), 3.12 (m, 4H, CH_2), 3.33 (m, 2H, CH_2), 4.09 (m, 2H, ester-CH_2), 5.00 (br, 1H, D_2O exchangeable, NH), 5.35 (br, 1H, D_2O exchangeable, NH), 6.12 (d, 1H, *J* 6.8 Hz, C4-H), 6.48 (m, 2H, ArH), 7.14-8.56 (m, 13H, ArH), 9.90 (br, 1H, D_2O exchangeable, NH). ^{13}C NMR (100 MHz, DMSO, 25 °C): δ 13.8, 17.4, 41.1, 44.9, 53.8, 58.6, 98.7, 116.5, 121.9, 124.1, 124.6, 126.4, 127.8, 133.2, 143.5, 146.8, 148.6, 149.2, 150.6, 151.5 and 164.1. ^{31}P NMR (162 MHz, DMSO, 25 °C): δ 14.15. Anal. Calcd. for $C_{36}H_{37}Cl_2N_8O_4P$: C, 57.84; H, 4.98; N, 14.99; Found: C, 58.10; H, 4.50; N, 14.37. MS: *m/z* 747 (M^+).

Ethyl 3-(bis((2-((7-chloroquinolin-4-yl)amino)ethyl)amino)phosphoryl)-6-methyl-2-oxo-4-phenyl-1,2,3,4-tetrahydropyrimidine-5-carboxylate (3a)

Yellow solid. Rf: 0.82 (60% methanol: ethyl acetate). Yield: 30%. M.p. 170 °C. FTIR (KBr): ν_{max} 1028, 1095, 1236, 1450, 1636, 1704, 2924, 3110, 3309 cm^{-1}. ^{1}H NMR (400 MHz, DMSO, 25 °C): δ 1.26 (t, 3H, *J* 7.1 Hz, CH_3), 1.42 (m, 2H, CH_2), 2.37 (s, 3H, C6-CH_3), 3.30 (m, 2H, CH_2), 3.50 (m, 2H, CH_2), 4.15 (m, 2H, ester-CH_2), 6.06 (d, 1H, *J* 5.9 Hz, C4-H), 6.25 (d, 1H, *J* 5.52 Hz, ArH), 6.36 (br, 1H, D_2O exchangeable, NH), 6.94- 7.04 (m, 4H, ArH), 7.35-7.43 (m, 3H, ArH), 7.95 (m, 2H, ArH), 8.45 (br, 1H, D_2O exchangeable, NH). ^{13}C NMR (100 MHz, DMSO, 25 °C): δ 13.8, 17.1, 29.8, 41.5, 42.8, 53.5, 58.1, 98.1, 117.2, 123.4, 124.1, 125.4, 126.2, 127.5, 133.6, 143.2, 146.9, 148.8, 150.4, 152.0 and 164.7. ^{31}P NMR (162 MHz, DMSO, 25 °C): δ 12.45. Anal. Calcd. for $C_{26}H_{28}Cl_2N_5O_4P$: C, 54.18; H, 4.90; N, 12.15; Found: C, 54.10; H, 4.59; N, 12.05. MS: *m/z* 575 (M^+).

Ethyl 3-(bis((3-((7-chloroquinolin-4-yl)amino)propyl)amino)phosphoryl)-6-methyl-2-oxo-4-phenyl-1,2,3,4-tetrahydropyrimidine-5-carboxylate (3b)

Off white solid. Rf: 0.48 (60% methanol: ethyl acetate). Yield: 63%. M.p. 105 °C. FTIR (KBr): ν_{max} 1026, 1098, 1235, 1454, 1642, 1701, 2948, 3116, 3404 cm^{-1}. ^{1}H NMR (400 MHz, DMSO, 25 °C): δ 1.13 (t, 3H, *J* 7.1 Hz, CH_3), 1.50 (m, 4H, CH_2), 2.24 (s, 3H, C6-CH_3), 2.62 (m, 2H, CH_2), 2.92 (m, 2H, CH_2), 3.16 (m, 4H, CH_2), 4.06 (m, 2H, ester-CH_2), 6.05 (d, 1H, *J* 6.6 Hz, C4-H), 6.38 (d, 1H, *J* 5.72 Hz, ArH), 6.49 (d, 1H, *J* 5.72 Hz, ArH), 7.19 (m, 3H, ArH), 7.34 (d, 2H, *J* 7.16 Hz, ArH), 7.41 (d, 2H, *J* 8.96 Hz, ArH), 7.56 (br, 1H, D_2O exchangeable, NH), 7.65 (br, 1H, D_2O exchangeable, NH), 7.76 (t, 2H, *J* 2.4 Hz, ArH), 8.23-8.37(m, 4H, ArH), 9.74 (br, 1H, D_2O exchangeable, NH). ^{13}C NMR (100 MHz, DMSO, 25 °C): δ 13.6, 17.0, 29.5, 41.2, 42.7, 53.6, 58.3, 98.5, 117.5, 123.9, 124.0, 125.4, 126.1, 127.3, 133.5, 143.1, 146.7, 148.9, 150.2, 151.8 and 164.6. ^{31}P NMR (162 MHz, DMSO, 25 °C): δ 14.65. Anal. Calcd. for $C_{38}H_{41}Cl_2N_8O_4P$: C, 58.80; H, 5.33; N, 14.45; Found: C, 58.74; H, 5.19; N, 14.27. MS: *m/z* 775 (M^+).

***In vitro* anti-plasmodial activity assay**

The samples were tested in triplicate on one or two separate occasions against CQ^S strain (D10) and CQ^R strain (Dd2) of *P. falciparum*. Continuous *in vitro* cultures of asexual erythrocyte stages of *P. falciparum* were maintained using a modified method of Trager and Jensen.[42] Quantitative assessment of antiplasmodial activity *in vitro* was determined via the parasite lactate dehydrogenase assay using a modified method described by Makler.[43]

The test samples were prepared to a 20 mg/ml stock solution in 100% DMSO and sonicated to enhance solubility. Samples were tested as a suspension if not completely dissolved. Stock solutions were stored at -20 ºC. Further dilutions were prepared on the day of the experiment. CQ was used as the reference drug in all experiments. Test samples were initially tested at three concentrations (10 µg/ml, 5 µg/ml and 2.5 µg/ml) to determine the starting concentration for the full dose-response assay. CQ was tested at three concentrations namely 30 ng/ml, 15 ng/ml and 7.5 ng/ml. A full dose-response was performed for all compounds to determine the concentration inhibiting 50% of parasite growth (IC_{50} value).

Test samples were tested at a starting concentration of 10 µg/ml, which was then serially diluted 2-fold in complete medium to give 10 concentrations; with the lowest concentration being 0.02 µg/ml. The same dilution technique was used for all samples. CQ was tested at a starting concentration of 1000 ng/ml. Several compounds were tested at a starting concentration of 1000 ng/ml. The highest concentration of solvent to which the parasites were exposed to had no measurable effect on the parasite viability (data not shown). The IC_{50} values were obtained using a non-linear dose-response curve fitting analysis via GraphPad Prism v.4.0 software.

Antiviral assays

The antiviral evaluation of the hybrids against HSV-1 wild-type or HSV-1 thymidine kinase deficient (TK^-, HSV-2, vaccinia virus and VSV was performed by seeding HEL 299 cells into 96-well dishes. For parainfluenza-3, reovirus-1, sindbis virus, CVB4 and punta toro virus, Vero cells were plated in 96-well dishes. FCV and FHV were evaluated on 96-well dishes seeded with CRFK cells. RSV, CVB4 and VSV were tested by plating HeLa cells into 96-well dishes. For influenza, MDCK cells were seeded. For all antiviral assays, dishes were incubated overnight at 37°C. Prior to infection, serial dilutions of the compounds were added to the cells. At 3 to 7 days post infection (depending on the virus), the virus-induced cytopathogenic effect was measured colorimetrically by the formazan-based MTS assay (CellTiter 96 Aqueous One Solution Cell Proliferation Assay from Promega), and the antiviral activity was expressed as the 50% effective concentration (EC_{50}). In parallel, the 50% cytotoxic concentration (CC_{50}) was derived from mock-infected HEL 299, Vero, CRFK, HeLa and MDCK cells. The activities were compared with reference compounds such as zanamivir, ribavirin, rimantadine, ribavirin, DS-10.000 and ganciclovir.

To test the activity of the hybrids against human cytomegalovirus (CMV) strains AD-169 and Davis, and varicella-zoster virus (VZV) TK^+ strain Oka and TK^- strain 07-1, confluent HEL cell cultures in microtiter 96-well plates were inoculated with 100 (CMV) or with 20 (VZV) plaque-forming units (PFU). After a 2-h virus adsorption period, residual virus was removed, and the cell cultures were incubated in the presence of varying concentrations of the test compounds in duplicate). Viral cytopathic effect (CMV) or viral plaque formation (VZV) was recorded as soon as it reached completion in the control virus-infected cell cultures that had not been treated with the test compounds, usually 5 days (VZV) and 7 days (CMV). Acyclovir and brivudin (VZV), and ganciclovir and cidofovir (CMV) were used as reference compounds.

Acknowledgements

KS is thankful to Guru Nanak Dev University, Amritsar for funding under RUSA II scheme. We thank Prof. Kelly Chibale and Prof. Peter Smith, University of Cape Town, South Africa for antiplasmodial testing of the compounds.

Keywords: Phosphoramide • Dihydropyrimidinione • Antiplasmodial • Molecular hybrids • Antiviral

[1] F. J. C. González, M. O. Sewe, A. M. Tompkins, H. Sjödin, A. Casallas, J. Rocklöv, C. Caminade, R. Lowe, *Lancet Planet Health* **2021**, *5*, 404–414.

[2] World Malaria Report **2021**. Geneva: World Health Organization, **2021**, (http://www.who.int/malaria/publications/).

[3] R. E. Howes, K. E. Battle, K. N. Mendis, D. L. Smith, R. E. Cibulskis, J. K. Baird, S. I. Hay, *Am. J. Trop. Med. Hyg.* **2016**, *95*, 15-34.

[4] R. W. Snow, *BMC Med.* **2015**, *13*, 23.

[5] M. A. Phillips, J. N. Burrows, C. Manyando, R. H. V. Huijsduijnen, W. C. V. Voorhis, T. N. C. Wells, *Nat. Rev. Dis. Primers* **2017**, *3*, 17050.

[6] J. Reader, M. E. Van der Watt, D. Taylor, C. L. Manach, N. Mittal, S. Ottilie, A. Theron, P. Moyo, E. Erlank, L. Nardini, N. Venter, S. Lauterbach, B. Bezuidenhout, A. Horatscheck, A. Van Heerden, N. J. Spillman, A. N. Cowell, J. Connacher, D. Opperaman, L. M. Orchard, M. Llinas, E. S. Istvan, D. E. Goldberg, G. A. Boyle, D. Calvo, D. Mancama, T. L. Coetzer, E. A. Winzeler, J. Duffy, L. L. Koekemoer, G. Basarab, K. Chiable, L. M. Birkholtz, *Nat. Commun.* **2021**, *12*, 269.

[7] L. C. Steinhardt, Y. S. Jean, D. Impoinvil, K. E. Mace, R. Weigand, C. S. Huber, J. S. F. Alexandre, J. Frederick, E. Nkurunziza, S. Jean, B. Wheeler, E. Doston, L. Slutsker, S. P. Kachur, J. W. Barnwell, J. F. Lemoine, M. A. Chang, *Lancet Glob. Health* **2017**, *5*, 96–103.

[8] M. Carins, S. J. Ceesay, I. Sagara, I. Zongo, H. Kessely, K. Gamougam, A. Diallo, J. S. Ogboi, D. Moroso, S. Van Hulle, T. Eloike, P. Snell, S. Scott, K. Bojang, J. B. Ouedraogo, A. Dicko, J. L. Ndiaye and P. Milligan, *PLoS Med.* **2021**, *18*, 1003727.

[9] G. Gachelin, P. Garner, E. Ferroni, J. P. Verhave, A. Opinel, *Malar. J.* **2018**, *17*, 96.

[10] Full Evidence Report on the RTS,S/AS01 Malaria Vaccine (https://www.who.int/immunization/sage/meetings/2015/october/1_Final_malaria_vaccine_background_paper_v2015_09_30.pdf).

[11] a) A. R. Sandoval and M. F. Bachmann, *Hum. Vaccin. Immun.* **2013**, *12*, 2558–2565. b) P. E. Duffy and J. P. Gorres, *npj Vaccines* **2020**, *5*, 48. (c) I. Mueller, A. R. Shakri and C. E. Chitnis, *Vaccine* **2015**, *33*, 7489-7495.

[12] A. Uwimana, N. Umulisa, M. Venkatesan, S. S. Svigel, Z. Zhou, T. Munyaneza, R. M. Habimana, A. Rucogoza, L. F. Moriarty, R. Sandford, E. Piercefield, I. Goldman, B. Ezema, E. Talundzic, M. A. Pacheco, A. A. Escalante, D. Ngamije, J. L. N. Mangala, M. Kabera, K. Munguti, M. Murindahabi, W. Brieger, C. Musanabaganwa, L. Mutesa, V. Udhayakumar, A. Mbituyumuremyi, E. S. Halsey, N. W. Lucchi, *Lancet Infect. Dis.* **2021**, *21*, 1120–1128.

[13] K. Haldar, S. Bhatttacharjee and I. Safeukui, *Brief. Funct. Genomics* **2018**, *16*, 156-170.

[14] R. W. Van der Pluijm, R. Tripura, R. M. Hoglund, A. P. Phyo, D. Lek, A. ul Islam, A. R. Anvikar, P. Satpathi, S. Satpathi, P. K. Behera, A. Tripura, S. Baidya, M. Onyamboko, N. H. Chau, Y. Sovann, S. Suon, S. Sreng, S. Mao, S. Oun, S. Yen, C. Amaratunga, K. Chutasmit, C. Saelow, R. Runcharern, W. Kaewmok, N. T. Hoa, N. V. Thanh, B. Hanboonkumupakam, J. J. Callery, A. K. Mohanty, J. Heaton, M. Thant, K. Gantait, T. Ghosh, R. Amato, R. D. Pearson, C.G. Jacob, S. Goncalves, M. Mukaka, N. Waithira, C. J. Woodrow, M. P. Grobusch, M. V. Vugt, R. M. Fairhurst, P. Y. Cheah, T. J. Peto, L. V. Seidlein, M. Dhorda, R. J. Maude, M. Winterberg, N. T. T. Nhien, D. P. Kwaitkowski, M. Imwong, P. Jittamala, K. Lin, T. M. Hlaing, K. Chotivanich, R. Huy, C. Fanello, E. Ashley, M. Mayxay, P. N. Newton, T. T. Hien, N. Valecha, F. Smithuis, S. Pukrittayakamee, A. Faiz, O. Miotto, J. Tarning, N. P. J. Day, N. J. White, A. M. Dondorp, *Lancet* **2020**, *395*, 1345–1360.

[15] a) I. Naidoo, C. Roper, *Trends Parasitol.* **2013**, *29*, 505-515. b) A. Uwimana, E. Legrand, B. H. Stokes, J. L. M. Ndikumana, M. Warsame, N. Umulisa, D. Ngamije, T. Munyaneza, J. B. Mazarati, K. Munuguti, P.

Campagne, A. Criscuolo, F. Ariey, M. Murindahabi, P. Ringwald, D. A. Fidock, A. Mbituyumuremyi, D. Menard, *Nat. Med.* **2021**, *27*, 1113-1115.

[16] a) B. Meuiner, *Acc. Chem. Res.* **2008**, 41, 69–77 b) N. J. White, *J. Clin. Invest.* **2004**, *113*, 1084-1092.

[17] K. Singh, H. Kaur, P. Smith, C. de Kock, K. Chibale, J. Balzarini, *J. Med. Chem.* **2014**, *57*, 435−448.

[18] P. Gupta, L. Singh, K. Singh, *Annu. Rep. Med. Chem.* **2019**, *53*, 73−105.

[19] L. Singh, D. Fontinha, D. Francisco, A. M. Mendes, M. Prudêncio, K. Singh, *J. Med. Chem*. **2020**, *63*, 1750-1762.

[20] K. Singh, T. Kaur, *Med. Chem. Commun.* **2016**, *7*, 749-768.

[21] M. Tripathi, D. Taylor, S. I. Khan, B. L. Tekwani, P. Ponnan, U. S. Das, T. Velpandian, D. S. Rawat, *ACS Med. Chem. Lett.* **2019**, *10*, 714−719.

[22] S. Dana, P. Valissery, S. Kumar, S. K. Gurung, N. Mondal, S. K. Dhar, P. Mukhopadhyay, *ACS Med. Chem. Lett*. **2020**, *11*, 1450−1456.

[23] F. W. Muregi, A. Ishih, *Drug Dev. Res.* **2010**, *71*, 20-32.

[24] a) K. Singh, K. Singh, *Adv. Heterocycl. Chem.* **2012**, *105*, 223-308. b) B. Schnell, U. T. Strauss, P. Verdino, K. Faber, C. O. Kappe, *Tetrahedron* **2000**, *56*, 1859-1862.

[25] a) K. Singh, D. Arora, E. Poremsky, J. Lowery, R. S. Moreland, *Eur. J. Med. Chem*. **2009**, *44*, 1997-2001. b) F. Bossert, H. Meyer, E. Wehinger, *Angew. Chem. Int. Ed. Engl.* **1981**, *20*, 762-769.

[26] O. Alam, S. A. Khan, N. Siddiqui, W. Ahsan, S. P. Verma, S. J. Gilani, *Eur. J. Med.Chem.* **2010**, *45*, 513−519.

[27] a) I. Graziadei, G. Zernig, R. Boer, H. Glossman, *Eur. J. Pharmacol.* **1989**, *172*, 329-337. b) Z. Cournia, L. Leng, S. K. Gandavadi, X. Du, R. Bucala, W. L. Jorgensen, *J. Med. Chem.* **2009**, *52*, 416–424.

[28] E. Klein, S. D. Bonis, B. Thiede, D. A. Skoufias, F. Kozielski, L. Lebeau, *Bioorg. Med. Chem.* **2007**, *15*, 6474–6488.

[29] a) C. O. Kappe, *Eur. J. Med. Chem*. **2000**, *35*, 1043. b) K. Singh, D. Arora, K. Singh, S. Singh, *Mini Rev. Med. Chem.* **2009**, *9*, 95. c) X. Zhu, G. Zhao, X. Zhou, X. Xu, G. Xia, Z. Zheng, L. Wang, X. Yang, S. Li, *Bioorg. Med. Chem. Lett.* **2010**, *20*, 299–301.

[30] N. Pagano, P. Teriete, M. Mattman, L. Yang, B. A. Snyder, Z. Cai, M. L. Heil, N. D. P. Cosford, *Bioorg. Med. Chem.* **2017**, *25*, 6248-6265.

[31] N. October, N. D. Watermeyer, V. Yardley, T. J. Egan, K. Ncokazi, K. Chibale, *ChemMedChem* **2008**, *3*, 1649 – 1653.

[32] a) C. McGuigan, K. Madela, M. Aljarah, C. Bourdin, M. Arrica, E. Barrett, S. Jones, A. Kolykhalov, B. Bleiman, K, D. Bryant, B. Ganguly, E. Gorovits, G. Henson, D. Hunley, J. Hutchins, J. Muhammad, A. Obikhod, J. Patti, C. R. Walters, J. Wang, J. Vernachio, C. V. S. Ramamurty, S. K. Battina, S. Chamberlain, *J. Med. Chem.* **2011**, *54*, 8632−8645. b) Y. Nan, Y. J. Zhang, *Front. Microbiol.* **2018**, *9*, 750.

[33] S. Lam, H. Chen, C. K. Chen, N. Min, J. J. H. Chu, *Sci. Rep.* **2015**, *5*, 12727.

[34] a) S. Pagola, P. W. Stephens, D. S. Bohle, D. Kosar, S. K. Madsen, *Nature* **2002**, *404*, 307–310. b) M. Foley and L. Tilley, *Int. J. Parasitol.* **1997**, *27*, 231-240.

[35] N. J. White, *Malar. J.* **2008**, *7*, S8.

[36] V. P. Sur, M. K. Sen, K. Komrskova, *Molecules* **2021**, *26*, 6199.

[37] K. Singh, H. Kaur, K. Chibale, J. Balzarini, *Eur. J. Med. Chem.* **2013**, *66*, 314−323.

[38] P. Gans, A. Sabatini, A. Vacca, *Talanta* **1996**, *43*, 1739-1753.

[39] a) A. Dorn, S. R. Vippagunta, H. Matile, C. Jaquet, J. L. Vennerstrom, R. G. Ridley, *Biochem. Pharmacol.* **1998**, *55*, 727-736. b) T. J. Egan, *J. Inorg. Biochem.* **2006**, *100*, 916-926.

[40] B. C. Croy, B. Over, F. Giordanetto, J. Kihlberg, *Chem. Biol.* **2014**, *21*, 1115-1142.

[41] D. K. Samy, B. G. Roy, J. R. Pereira, J. Neyts, S. Nanjappan, S. Maity, M. Mookerjee, L. Naesens, *Bioorg. Med. Chem. Lett.* **2017**, *27*, 139–142.

[42] W. Trager, J. B. Jensen, *Science* **1976**, *193*, 673-675.

[43] M. T. Makler, J. M. Ries, J. A. Williams, J. E. Bancroft, R. C. Piper, B. L. Gibbins, D. J. Hinrichs, *Am. J. Trop. Med. Hyg.* **1993**, *48*, 739−741.

Entry for the Table of Contents

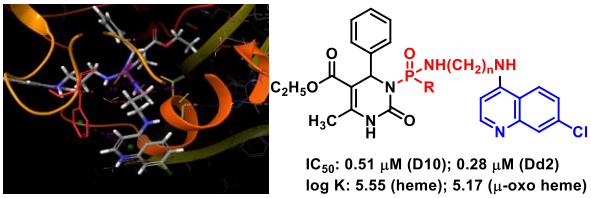

Antiplasmodial activity, *in silico* docking in the binding pockets of dihydrofolate reductase, heme binding, ADMET properties, and antiviral properties of a new set of quinolone-dihydropyrimidinone hybrids is presented. Compounds showed moderate to good antiplasmodial activity against chloroquine sensitive (D10) and resistant (Dd2) strains of *Plasmodium falciparum*.